Journal of Sound and Vibration (1999) **220**(1), 135–154
Article No. jsvi.1998.1942, available online at http://www.idealibrary.com on IDEAL

AN APPROACH FOR EVALUATING POWER TRANSFER COEFFICIENTS FOR SPOT-WELDED JOINTS IN AN ENERGY FINITE ELEMENT FORMULATION

N. VLAHOPOULOS AND X. ZHAO

Department of Naval Architecture and Marine Engineering,
The University of Michigan, *Ann Arbor*, *MI* 48109-2145, *U.S.A.*

AND

T. ALLEN

Ford Research Laboratory, *Ford Motor Company*, *Dearborn*, *MI*, *U.S.A.*

(*Received* 16 *February* 1998, *and in final form* 31 *August* 1998)

Low levels of vibration and noise in vehicles contribute to raising their perceived value. Currently, a widely utilized approach for high frequency analysis in the vibro–acoustics area is the Statistical Energy Analysis. An emerging new technology is the Energy Finite Element Analysis (EFEA). The energy density constitutes the primary variable in EFEA. The governing differential equations are formulated with respect to the energy density. A finite element approach is employed to solve numerically the governing equations. In order for this new method to be applicable to automotive structures it is important to identify an approach for modelling spot-welded joints. This paper presents the development, implementation, and validation of a numerical process that evaluates the EFEA power transfer coefficients that correspond to spot-welded joints. These power transfer coefficients can be utilized in an EFEA model to simulate the behavior of the spot-welded connections.

1. INTRODUCTION

The vibro–acoustics attributes of a vehicle are important in its perceived value and its competitiveness. Simulation technology is utilized for predicting and improving these characteristics [1–6]. Currently, the simulation capabilities are based on methods suitable for low frequencies (finite element and boundary element methods [1–4]), and methods applicable to high frequency analysis (statistical energy analysis) [5, 6]. The frequency range where there is a small number of waves (usually four or five) within each component of a system is characterized as low frequency range. Numerical methods which compute the discrete frequency and space displacement of noise levels are suitable for analysis at low frequencies. As the number of waves within each member increases, a larger number of elements

0022–460X/99/060135 + 20 $30.00/0

is required in the finite element and boundary element numerical models to capture the response accurately. When the frequency of excitation becomes high enough so that the vibrational energy in all the members can be considered to be in the reverberant field, the corresponding range is characterized as high frequency [7]. Statistical Energy Analysis (SEA) has been developed and utilized in naval, aerospace, and automotive applications for high frequency vibro–acoustics simulations [5–10]. The SEA is based on modelling a system as an assembly of groups of similar modes (subsystems). The total amount of energy stored in all the modes of a subsystem averaged over a frequency band constitutes a single lumped parameter representing the behavior of each subsystem. The amount of the energy stored within each subsystem, the amount of power transferred between subsystems, and the amount of power dissipated from each subsystem, depend on the modal density of the subsystems, their damping, and their connectivity. The SEA solution provides information about the amount of energy stored in each subsystem. The SEA results can be utilized to determine the path of power flow through a system, and determine appropriate damping treatment. An emerging method for high frequency simulations is the Energy Finite Element Analysis (EFEA). The energy density, time averaged over a period, and space averaged over a wavelength, consitutes the primary variable in the EFEA formulation [11–15]. A numerical solution to the EFEA governing differential equations is accomplished by a finite element formulation [14]. The SEA formulation is derived by viewing the vibration of a system from a modal point, and the EFEA is developed by considering the vibration from a wave perspective. The attractive characteristics of the EFEA are: (1) it allows ready utilization of numerical models developed for low frequency computations; (2) it provides information for the response on a discrete element basis rather than as a lumped parameter over an entire subsystem; (3) it allows damping to be prescribed on a local basis on each individual element rather than as a lumped quantity over the entire subsystem.

In EFEA, the power transferred between different components is handled by a specialized joint formulation [14]. The power transmissibility characteristics between members are considered to demonstrate the same behavior as semi-infinite members with the same properties and connected in the same manner. Power transfer coefficients (reflection and transmission coefficients) between members are computed from the semi-infinite solutions and utilized to develop a relationship between power flow and energy density at a joint. This relationship is utilized to formulate the coupling between fully connected members in EFEA. In order to expand the applicability of the EFEA into automotive applications it is critical to be able to include spot-welded joints in an EFEA numerical model, since spot-welding is widely utilized in the car body manufacturing process.

In the past, conventional finite element analysis was utilized to generate power transmissibility information for members with continuous connections. Artificial damping was imposed in all members in order to eliminate reflections from their boundaries. Then, SEA coupling loss factors were derived based on the power transmissibility information produced by the conventional finite element analysis [16–20]. The work presented in this paper is based on a similar concept of utilizing conventional finite element models to compute the coupling

characteristics of a spot-welded joint, and then determining the corresponding EFEA power transfer coefficients that can be employed in an EFEA model for high frequency analysis. The following new elements are presented:

(1) Conventional finite element models of spot-welded or continuously connected members are utilized to compute the ratio of the stored energy between receiving and externally excited members. In this formulation there is no requirement for artificial damping to be introduced in the system in order to eliminate reflections from the boundaries. Thus, the energy ratio is computed based on the total energy stored in each member. The energy ratio constitutes the variable that characterizes the connection.

(2) An iterative algorithm is developed for computing the EFEA power transfer coefficients for spot-welded members based on the ratio of total energy distributed among members. The development of this specialized algorithm is necessary because the energy ratio includes information for the power reflected from the boundaries of each member.

(3) The new algorithms are implemented into software.

(4) The new numerical developments are utilized to analyze members connected by a continuous joint and the EFEA results are compared to test data and results from the literature.

(5) The new numerical developments are utilized to analyze members connected by two different spot-welding patterns and the EFEA results are compared to test data.

2. MATHEMATICAL FORMULATION

In order to present the current development some background information will be given about the EFEA method, and the existing formulation for modelling continuous joints. Although a variety of members (rods, beams, plates, acoustic spaces) can be represented in EFEA [12–15], only the formulation associated with the flexural degree of freedom of a plate will be discussed here. It comprises the foundation for developing technology for modelling the spot-welded joints between plate members.

2.1. MATHEMATICAL BACKGROUND ON THE EFEA FORMULATION

The development of the governing differential equation is based on the farfield solution for the out-of-plane deflection of a plate:

$$w(x, t) = (A_x \, e^{-ik_x x} + B_x \, e^{ik_x x})(A_y \, e^{-ik_y y} + B_y \, e^{ik_y y}) \, e^{i\omega t}, \tag{1}$$

where A_x, B_x, A_y, B_y are constants associated with the amplitudes of the propagating wave in the positive and negative x and y direction respectively, and k_x, k_y are components of the wavenumber associated with the damped frequency of oscillation in the x and y directions. $w(x, t)$ constitutes the far field solution for the out of plane displacement equation for a plate:

$$D\nabla^4 w + \rho h \, \partial^2 w / \partial t^2 = F(x, t), \tag{2}$$

where $D = Eh^3/12(1 - v^2)$ is the rigidity of the plate, v is Poisson's ratio, h is the thickness of the plate, ρ is density of the plate, and $F(x, t)$ is the external out of plane load applied on the plate. The energy density constitutes the primary variable in formulating the governing differential equation. The energy density averaged over a period can be expressed in terms of the far field displacement solution [12]:

$$\langle e \rangle = \left\langle \frac{D}{4}\left[\frac{\partial^2 w}{\partial x^2}\left(\frac{\partial^2 w}{\partial x^2}\right)^* + \frac{\partial^2 w}{\partial y^2}\left(\frac{\partial^2 w}{\partial y^2}\right)^* + 2v\,\frac{\partial^2 w}{\partial x^2}\left(\frac{\partial^2 w}{\partial y^2}\right)^* \right.\right.$$

$$\left.\left. + 2v(1 - v)\,\frac{\partial^2 w}{\partial x\,\partial y}\left(\frac{\partial^2 w}{\partial x\,\partial y}\right)^*\right] + \frac{\rho h}{4}\,\frac{\partial w}{\partial t}\left(\frac{\partial w}{\partial t}\right)^* \right\rangle, \tag{3}$$

where * indicates complex conjugate, and $\langle\ \rangle$ indicates time averaging over a period (i.e., $\langle A \rangle = (1/T)\int_t^{t+T} A(\tau)\,\mathrm{d}\tau$). The two intensity components averaged over a period are also associated with the far field displcement solution as

$$\langle I_{xx} \rangle = \left\langle D\left(\frac{\partial^2 w}{\partial x^2} + v\,\frac{\partial^2 w}{\partial y^2}\right)\left(\frac{\partial^2 w}{\partial x\,\partial t}\right)^* + D(1 - v)\,\frac{\partial^2 w}{\partial x\,\partial y}\left(\frac{\partial^2 w}{\partial y\,\partial t}\right)^* \right.$$

$$\left. - D\,\frac{\partial}{\partial x}\,\nabla^2 w\left(\frac{\partial w}{\partial t}\right)^* \right\rangle,$$

$$\langle I_{yy} \rangle = \left\langle D\left(\frac{\partial^2 w}{\partial y^2} + v\,\frac{\partial^2 w}{\partial x^2}\right)\left(\frac{\partial^2 w}{\partial y\,\partial t}\right)^* + D(1 - v)\,\frac{\partial^2 w}{\partial x\,\partial y}\left(\frac{\partial^2 w}{\partial x\,\partial t}\right)^* \right.$$

$$\left. - D\,\frac{\partial}{\partial y}\,\nabla^2 w\left(\frac{\partial w}{\partial t}\right)^* \right\rangle, \tag{4}$$

where $\langle I_{xx} \rangle$, $\langle I_{yy} \rangle$ are the two time averaged intensity components. The far field displacement (1), can be substituted in equations (3) and (4). By integrating the new expressions over one wavelength, equations can be derived for the time and space averaged energy density and intensity components $\langle \underline{e} \rangle$, $\langle \underline{I}_{xx} \rangle$, $\langle \underline{I}_{yy} \rangle$ respectively, where _ indicates space averaging over a wavelength. From these expressions a relationship can be derived as

$$\langle \vec{\underline{I}} \rangle = -(c_g^2/\eta\omega)\nabla\langle \underline{e} \rangle, \tag{5}$$

where η is the hysterisis damping factor, and c_g the group speed defined as (see reference [21])

$$c_g = \mathrm{d}\omega/\mathrm{d}k = 2[\omega^2 D/\rho h]^{1/4}, \tag{6}$$

where ω is the frequency in rad/s. The time and space averaged dissipated power $\langle \underline{\Pi}_{\text{diss}} \rangle$ can be related to the corresponding energy density as (reference [16])

$$\langle \underline{\Pi}_{\text{diss}} \rangle = \eta\omega \langle \underline{e} \rangle. \tag{7}$$

By considering an energy balance results in (from references [12, 13])

$$\langle \underline{\Pi}_{\text{in}} \rangle = \langle \underline{\Pi}_{\text{diss}} \rangle + \nabla \langle \vec{\underline{I}} \rangle, \tag{8}$$

where $\langle \underline{\Pi}_{\text{in}} \rangle$ corresponds to the input power. Then substituting equations (5) and (7) into equation (8), results in the governing differential equation for the time and space averaged energy density:

$$-(c_g^2/\eta\omega)\nabla^2 \langle \underline{e} \rangle + \eta\omega \langle \underline{e} \rangle = \langle \underline{\Pi}_{\text{in}} \rangle. \tag{9}$$

This constitutes the governing differential equation for the EFEA. A finite element approach [14, 15] is employed for solving it numerically.

2.2. FINITE ELEMENT FORMULATION

The element matrices are derived from the weak variational form of equation (9):

$$-\int_{C_e} \frac{c_g^2}{\eta\omega} \phi \hat{n} \nabla \langle \underline{e} \rangle \, \mathrm{d}C_e + \int_{S_e} \frac{c_g^2}{\eta\omega} \nabla \phi \nabla \langle \underline{e} \rangle \, \mathrm{d}S + \int_{S_e} \eta\omega\phi \langle \underline{e} \rangle \, \mathrm{d}S$$

$$- \int_{S_e} \phi \langle \underline{\Pi}_{\text{in}} \rangle \, \mathrm{d}S = 0, \tag{10}$$

where ϕ is an arbitrary function, C_e is the boundary of the element, S_e is the surface of the element, and $\hat{n}$ is the unit vector normal to the element boundary. By utilizing shape functions within each element, and representing all variables as a linear superposition of the shape functions and the nodal values, a system of linear equations can be produced:

$$[\mathbf{K}^e]\{\mathbf{e}^e\} = \{\mathbf{F}^e\} + \{\mathbf{Q}^e\}, \tag{11}$$

where $\{\mathbf{e}^e\}$ is the vector of nodal values for the time and space averaged energy density for a finite element, $[\mathbf{K}^e]$ is the system matrix for each finite element, $\{\mathbf{F}^e\}$ is the excitation vector representing the energy input at each node of the finite element, and $\{\mathbf{Q}^e\}$ is the power flow across the element boundary. Representative terms for the matrix and the excitation vectors can be written as

$$K_{ij}^e = \int_{S_e} \left(\frac{c_g^2}{\eta\omega} \nabla N_i \nabla N_j + \eta\omega N_i N_j \right) \mathrm{d}S, \qquad F_i^e = \int_{S_e} N_i \langle \underline{\Pi}_{in} \rangle \, \mathrm{d}S,$$

$$Q_i^e = -\int_{C_e} N_i \hat{n} \langle \vec{\underline{I}} \rangle \, \mathrm{d}C_e, \tag{12}$$

where N_i are shape functions, and $\langle \vec{\underline{I}} \rangle$ is the time and space averaged intensity at the boundary of the element. In order to derive the Q_i^e terms, the relationship between energy density and intensity (equation (5)) is employed. Using equation (5), the power flow at the boundary of an element can be expressed in terms of the nodal values of the energy density at the same location. Q_i^e provides the mechanism for connecting elements together across discontinuities. At the joint locations the energy density is discontinuous, and coupling is achieved through continuity of power flow.

2.3. FORMULATION OF JOINTS

In the conventional finite element formulations the continuity of the primary variables of the analysis at the nodes between elements is utilized in order to assemble the global system matrix. In the EFEA the continuity condition applies to the energy density only when geometry and material properties do not change. At positions where different members are connected, or at locations of discontinuities within a single member, the energy density is discontinuous. The corresponding boundary between the elements defines a joint location. A specialized approach is developed in order to formulate the connection between the discontinuous primary variables at the joints. The continuity of power flow across a joint and the corresponding equations are employed in the development. The vector $\{\mathbf{Q}^e\}$ is derived as a product of a matrix representing the power flow mechanism across the joint ($[\mathbf{ET}_j^i]$) and the nodal values of the energy density [14].

In order to derive the power transfer coefficients and sequentially formulate the entries of the power transfer matrix $[\mathbf{ET}_j^i]$, the connected members are considered semi-infinite and fully attached to each other [21]. The connection is considered massless, rigid (does not change in shape), without power loss, and infinite in length. These assumptions in the formulation of the joints are valid for the high frequency range which is consistent with the overall EFEA formulation since only the far field displacement solutions are utilized in deriving expressions for the energy density and the intensity (equations (3) and (4)). The equations relating the nodal values of the power flow and the nodal values of the energy density can be written as (see reference [14])

$$\begin{Bmatrix} Q_n^i \\ Q_{n+1}^i \\ Q_m^j \\ Q_{m+1}^j \end{Bmatrix} = [\mathbf{ET}_j^i] \begin{Bmatrix} e_n^i \\ e_{n+1}^i \\ e_m^j \\ e_{m+1}^j \end{Bmatrix}, \tag{13}$$

where n and $(n+1)$ indicate the two nodes of the ith element at the joint, and m, $(m+1)$ indicate the two nodes of the jth element at the joint, and $[\mathbf{ET}_j^i]$ is a matrix representing the power transfer mechanism. The power transfer coefficients are utilized to calculate the terms of matrix $[\mathbf{ET}_j^i]$. The power transfer coefficients are computed from analytical solutions of semi-infinite members fully connected to each other, and by taking into account the continuity of the power flow across

the joint. By taking into account equation (13) the finite element equations for elements i and j (equation (11)) result in

$$\left[\begin{bmatrix}[\mathbf{K}^{ei}] & \\ & [\mathbf{K}^{ej}]\end{bmatrix} + [\mathbf{CET}_j^i]\right]\begin{Bmatrix}\mathbf{e}^i \\ \mathbf{e}^j\end{Bmatrix} = \begin{Bmatrix}\mathbf{f}^i \\ \mathbf{f}^j\end{Bmatrix}, \tag{14}$$

where $[\mathbf{K}^{ei}]$, $[\mathbf{K}^{ej}]$ are the element matrices for the ith and jth element, $\{\mathbf{e}^j\}$, $\{\mathbf{e}^j\}$ are vectors containing all the nodal degrees of freedom for elements i, j respectively, and $[\mathbf{CET}_j^i]$ is a coupling matrix consisting of the coefficients of $[\mathbf{ET}_j^i]$ positioned in the appropriate locations.

2.4. DERIVATION OF THE ENERGY TRANSFERRED BETWEEN SPOT-WELDED MEMBERS

Due to the discontinuous nature of a spot-welded connection the current analytical approach of determining the power transfer coefficients and deriving the entries of the coupling matrices at the joints is not applicable. A concept of employing conventional finite element models to calculate the energy in structural members, and then utilizing the energy ratio between members to calculate SEA coupling loss factors has been developed in the past [16–20]. Specifically, SEA coupling loss factors have been computed through finite element calculations for the following cases: (1) assemblies of fully connected plates [16, 17], (2) beam junctions [19], (3) interfaces between structural and acoustic subsystems [18], (4) capturing the resonant characteristics of coupled subsystems [20].

It has been observed that in high frequencies a conventional finite element model cannot compute, in a reliable manner, the vibration at some specific point and for some specific frequency. However, if the results are averaged over the surface of each structural member and over a frequency band, then the values for the energy ratio between members are reliable [16, 17]. It has also been indicated that approximately six wave lengths are required for the finite element computations to provide reliable energy ratio data [16]. The averaged energy data computed by the finite element method are reliable because although the natural frequency might be shifted in the high frequency range, the shapes of the normal modes are still captured. Therefore, the frequency and space averaged finite element results are reliable [16, 17]. In all the previous work where conventional finite element models were utilized to compute SEA coupling loss factors, artificial damping was introduced in the FEA model to eliminate reflections from the boundaries [16, 17, 19]. Thus, the finite element model with the artificial damping approximates an assembly of semi-infinite members. The reason for relying on conventional finite element analysis to extract the characteristics of the power transfer for a SEA analysis, is the flexibility of the finite element method in modelling complex connections which cannot be accounted by analytical solutions.

A similar overall approach is employed in the work presented in this paper. The conventional finite element method is utilized to compute power transfer characteristics for spot-welded connections. No artificial damping is introduced in the finite element models in this case. Instead, a numerical iterative algorithm is developed that processes the data computed by the finite element analysis, and

calculates the power transfer coefficients that can represent the spot-welded connections in high frequency EFEA models. The task of formulating the spot-welded joints in EFEA is divided into two steps. First, a finite element model is constructed to characterize the power transfer mechanism associated with a particular spot-welding connection. Members connected by the spot-welding pattern that is analyzed are modelled with finite elements. A forced frequency response analysis is performed over several frequencies within each frequency band where the power transfer characteristics are to be computed. The ratio of the frequency averaged kinetic energy between the members is utilized to characterize the power transfer mechanism of the particular spot-welding connection. Then, the ratio of the kinetic energies is processed by an iterative algorithm and the corresponding EFEA power transfer coefficients are computed. Finally, the entries of the power transfer matrix $[\mathbf{ET}_j]$ are calculated from the power transfer coefficients. The outlined process and the corresponding software that performs the computation of the power transfer coefficients are general and can handle any type of spot-welded connection. The process must be repeated for every different spot-welding pattern that is being modelled, because the ratio of the kinetic energies computed by the finite element analysis is expected to change depending on the characteristics of each spot-welded connection.

The general purpose finite element code NASTRAN [22] is utilized for the finite element analysis. A finite element model for the spot-welded connection and the corresponding members must be created. A direct frequency response solution must be performed at every frequency of analysis. The direct analysis relaxes the requirement of six elements per wavelength, since the normal modes are not computed explicitly. The complete mass, stiffness, and damping matrices are employed in the direct solution, therefore no errors from modal truncation are introduced in the analysis. The EFEA approach is applicable for simulations in the high frequency range, and for automotive applications the targeted range of applicability is between 800–2500 Hz. Therefore, the computations are concentrated in the 1/3 octave frequency bands between 800 Hz and 2500 Hz. The finite element direct frequency response analysis can be performed at 2·5 Hz increments for the frequency bands with center frequencies at 800 Hz, 1000 and 1250 Hz, and at increments of 5 Hz for the bands with center frequencies at 1600, 2000 and 2500 Hz. The analyses for each band are performed separately. The finite element results for the vibration velocities are contained in a NASTRAN ".pch" file format. A computer code is developed for processing the finite element results and generating information for the ratio of the kinetic energy between the receiving and the excited members. The computational process is outlined in Figure 1. The algorithm and the software are general enough that there are no restrictions on the type of structural connections (spot-welded or continuous connection) or number of members to be processed. A characteristic zone is defined over each member of the finite element model and it can contain the entire member or a section of it. Computations are performed over each characteristic zone to calculate the amount of kinetic energy present within it. The ratio of energy between zones associated with different members is utilized to represent the power transfer characteristics of the connection. A separate file in NASTRAN format

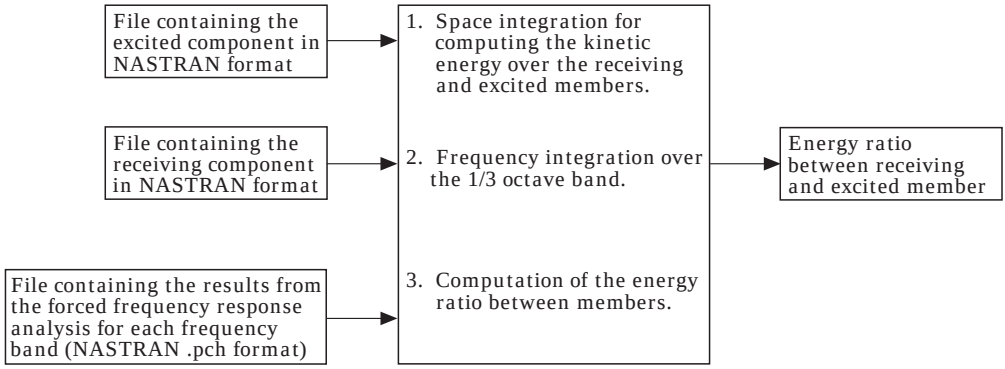

Figure 1. Numerical process for computing the energy ratio between a receiving and an excited member.

is required to define each zone of the finite element model over which the kinetic energy will be computed for each excited or receiving member. The zone over which the energy will be computed can be comprised by either the entire member, or a characteristic section of the member. From the data defining each zone the area and the material properties (thickness and density) are determined. The normal velocity is first computed over each finite element that belongs to a characteristic zone as

$$v_{n_E} = \int_{S_E} \tilde{v}\hat{n}\, \mathrm{d}A \Big/ \int_{S_E} \mathrm{d}A, \tag{15}$$

where subscript E indicates an element quantity, $\tilde{v}$ is the complex structural velocity, $\hat{n}$ is the unit normal over the element, v_{n_E} is the value of normal velocity for each element, and S_E is the element surface. Then, the kinetic energy over the surface of each representative zone of every member is computed for each frequency of analysis as

$$KE_{Zm} = \tfrac{1}{2} \int_{S_{Zm}} \rho_m t_m v_{n_{Em}}^2\, \mathrm{d}A, \tag{16}$$

where KE_{Zm} is the kinetic energy stored in the zone representing the mth member, S_{Zm} is the associated surface, ρ_m is the material density and t_m is the local thickness of the member. The results for all the frequencies in each frequency band are averaged for each member by taking their summation resulting in $\Sigma_{f_i} KE_{Zm}$. The latter represents the energy stored within the representative zone of the mth member for the 1/3 octave band with center frequency f_i. Finally, the energy ratio is computed as

$$(ER)_m^l = \sum_{f_i} KE_{Zl} \Big/ \sum_{f_i} KE_{Zm}, \tag{17}$$

where $(ER)_m^l$ is the energy ratio between the lth and the mth structural components. All the energy ratios are generated between the excited (mth) and the

receiving (lth) members. The benefit of this averaging technique is that it can account for local characteristics of the connection between the structural members. The local characteristics are captured because a conventional finite element model is utilized to represent the connection and the members. The energy ratios between members of the spot-welded connection are utilized to compute the EFEA power transfer coefficients, and generate the power joint matrices of the EFEA formulation.

2.5. DERIVATION OF EFEA POWER TRANSFER COEFFICIENTS FROM THE ENERGY RATIO INFORMATION

In previous work when the energy ratio computed by a finite element analysis was processed to evaluate SEA coupling loss factors between plates, a simple relationship was utilized [references 16, 17]:

$$\eta_{jk} = (c_{gj} L / 2\eta^2 f A_j)\tau, \tag{18}$$

where η_{jk} is the coupling loss factor between subsystems j and k, c_{gj} is the group speed in the excited member, L is the length of the junctions between the plates, A_j is the area of the excited plate, f is the frequency where the coupling loss factor is computed, τ is the energy ratio between receiving and excited member and η is the damping coefficient for the excited system. Equation (18) is a formula utilized primarily in computing the coupling loss factor from measured energy ratios. The set up which is utilized to compute the energy ratio τ of equation (18) must contain sufficient damping applied at the edges of the receiving members in order to avoid reflections from the boundaries. The damping must be introduced artificially on the receiving members by applying viscoelastic treatment at their boundaries [16]. The artificial damping requirement increases the complexity of the set up and introduces uncertainty. In this work artificial damping is not imposed on any members, and thus the set up remains simple. The energy in each member corresponds to a reverberant field since the reflections from the boundaries are not damped. Instead, an iterative algorithm is created in order to compute the EFEA power transfer coefficients from results obtained from the finite element models without artificial damping. The development of the iterative algorithm is preferred rather than attempting to introduce artificial damping in the finite element model for two reasons:

(1) The modelling becomes simpler and uncertainties associated with imposing artificial damping are eliminated.

(2) The iterative algorithm can be utilized to extract EFEA power coefficients regardless of whether the energy ratio information is produced by a finite element analysis or from actual testing. In case that the energy ratio is produced by a test, the iterative algorithm eliminates the requirement for artificial damping and simplifies significantly the test set up.

Due to the presence of reflections from the boundaries of the members, there are four mechanisms responsible for the energy stored within the excited member; input power, power reflected back from the joint, power reflected from the boundaries and power transmitted from the receiving member back to the excited

one due to the small amount of damping present in the receiving member. In the receiving member there are three mechanisms associated with the stored energy; power transmitted from the excited member, power reflected from the boundaries, and power reflected back from the joint.

For a spot-welded joint both the reflection and the transmission (power transfer) coefficients will change from the original values corresponding to a fully connected joint of similar characteristics. The new values should be such that the EFEA solution results in the same amount of reverberant energy stored within each component as either is evaluated by the averaging finite element approach or possibly measured through testing. From reciprocity considerations the entries associated with the power transfer coefficients of the flexural waves contained in matrix $[\mathbf{CET}_j^i]$ (equation (14)) can be expressed in terms of the transmission τ_{ij} and the reflection r_{ii} coefficients. By concentrating on the power transfer coefficients associated only with the energy of flexural waves, the summation of $\tau_{ij} + r_{ii}$ remains constant between fully connected and spot-welded joints of similar structural characteristics. Therefore, the two coefficients can be reduced to one unknown constant r. The system of the EFEA equations for the members connected at the joint can be written as

$$\left[\begin{bmatrix} K_l & \\ & K_m \end{bmatrix} + [\mathbf{CJ}_m^l(r)]\right]\begin{Bmatrix}\mathbf{e}_l \\ \mathbf{e}_m\end{Bmatrix} = \begin{Bmatrix}\mathbf{f}_l \\ \mathbf{f}_m\end{Bmatrix} \Rightarrow [\mathbf{SK}(r)]\begin{Bmatrix}\mathbf{e}_l \\ \mathbf{e}_m\end{Bmatrix} = \begin{Bmatrix}\mathbf{f}_l \\ \mathbf{f}_m\end{Bmatrix} \Rightarrow \begin{Bmatrix}\mathbf{e}_l(r) \\ \mathbf{e}_m(r)\end{Bmatrix}, \quad (19)$$

where subscripts l, m indicate the lth and mth members respectively, $[\mathbf{SK}(r)]$ is the system matrix including the joint matrices, represented as a function of the unknown power transfer constant. From processing the results of the finite element analysis the energy ratio $(ER)_m^l$ between the lth receiving member and mth excited member is computed. The equivalent expression from the EFEA formulation can be expressed as a function of the unknown power transfer coefficient r as

$$ER_m^l(r) = \sum_{j=1}^{L} e_{lj}(r) S_{lj} t_{lj} \Big/ \sum_{i=1}^{M} e_{mi}(r) S_{mi} t_{mi}, \quad (20)$$

where M and L are the total number of elements in the mth and lth members respectively, t_{mi}, t_{lj} are the thicknesses associated with the ith element of the mth member and the jth element of the lth member, respectively, e_{mi}, e_{lj} are the energy densities associated with the ith element of the mth member and the jth element of the lth member, respectively, and S_{mi}, S_{lj} are the corresponding element areas. Combining equations (17) and (20) results in

$$ER_m^l(r) = (ER)_m^l. \quad (21)$$

An iterative approach is utilized for obtaining solutions to this equation [24]. The EFEA power transfer coefficients representing the spot-welded connections

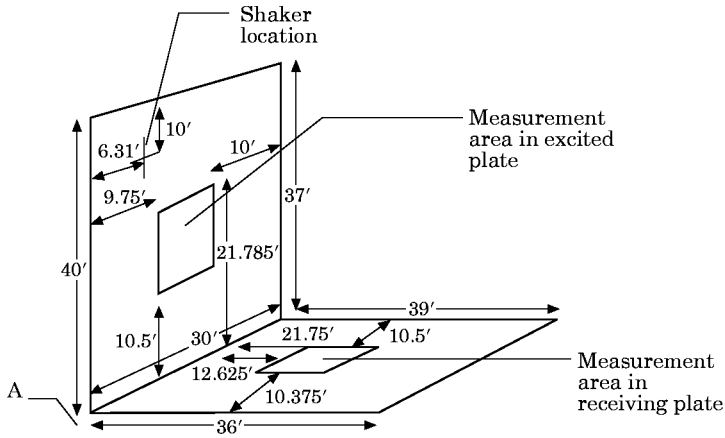

Figure 2. Test set up. All dimensions in inches.

are computed from the iterative solution. The algorithm is based on the equation

$$\frac{ER_m^l(r)^{(n+1)} - (ER)_m^l}{ER_m^l(r)^{(n+1)} - ER_m^l(r)^{(n)}} = \frac{r^{(n+1)} - r}{r^{(n+1)} - r^{(n)}} \Rightarrow r$$

$$= r^{(n+1)} - [r^{(n+1)} - r^{(n)}] \frac{ER_m^l(r)^{(n+1)} - (ER)_m^l}{ER_m^l(r)^{(n+1)} - ER_m^l(r)^{(n)}}, \tag{22}$$

where superscripts n, $(n+1)$ represent the consecutive iteration steps. The original values of the power transfer coefficients of a continuous joint with similar structural properties are utilized in defining the initial value for coefficient r (i.e. $r^{(1)}$). A value modified by a 10% change can be employed in defining the complete set of initial conditions (i.e., $r^{(2)} = 1{\cdot}1r^{(1)}$). Equations (19) and (20) are utilized for computing the values of $ER_m^l(r)$ for each increment. The algorithm is considered to converge when the difference

$$(ER_m^l(r) - (ER)_m^l)/(ER)_m^l < UL \tag{23}$$

is smaller than a user defined limit UL. The iterative algorithm is independent whether the targeted value $(ER)_m^l$ is specified by a finite element direct frequency response analysis or by testing. The development of the iterative process simplifies both the finite element model and the test set up that can be utilized to evaluate the ratio of energies between receiving and excited members, since it eliminates the requirement of artificial damping.

3. VALIDATION, APPLICATIONS

Three pairs of plates are constructed and tested in order to validate this development. The energy ratio between receiving and excited plates is computed first by conventional FEA methods, and the averaging algorithms and software developed in this work. The energy ratio is utilized by the developed iterative algorithm to compute the corresponding EFEA power transfer coefficients. The

latter are introduced into an EFEA model and the energy ratio between the receiving and the excited member are computed by an EFEA analysis and compared to test data. The dimensions of the plates, the measurement areas, and the location where the excitation is applied are presented in the Figure 2. The plates are constructed from low carbon steel, 0·03 in. thick having 0·25% structural damping. The dimensions are selected to be uneven in order to create a diffused field in both members. In an actual structure the diffused field will be created by the irregularities at the boundaries of the individual members. The three assemblies have fully welded, spot-welded at 2 in. intervals, and spot-welded at 4 in. intervals, joint connections. Although the primary interest is in modelling the spot-welded connections, a pair of fully connected plates is also tested and analyzed since results for plates connected at a right angle are available in the literature [17, 25–27]. Correlation between the trends in the test data and numerical results produced in this work and published data for the fully connected plates establishes confidence in the experimental and analytical results presented in this paper. In addition it demonstrates that the developed approach can compute with increased accuracy the power transfer coefficients for fully connected members over the analytical approach that utilizes solutions for semi-infinite members. During testing each plate assembly is suspended by flexible cords in order to present free boundary conditions at all edges. Two measurement areas, one for each plate (Figure 2), are scanned with a laser vibrometer. Measurements are collected at 100 points for each measurement area. The measurements are processed by adding the squares of the velocities over each area, and then taking a summation over frequencies for each 1/3 octave frequency band. Since the thickness for both plates is the same, the mass corresponding to each measurement section can be determined from the corresponding area. The ratio of the kinetic energies between the two measurement areas of the two plates is computed for each frequency band as

$$\left(\sum_{i=1}^{I}\sum_{n=1}^{100} A_{1n} v_{1ni}^2\right) \Big/ \left(\sum_{i=1}^{I}\sum_{n=1}^{100} A_{2n} v_{2ni}^2\right), \tag{24}$$

where A_{1n}, A_{2n} are the areas corresponding to each measurement point of the receiving and the excited plate respectively, v_{1ni}, v_{2ni} are the measured velocities at the nth point of the receiving and the excited plate respectively, and I is the total number of frequencies within each 1/3 octave band. Test data are collected at 2·5 Hz increments for the 1/3 octave bands with center frequencies at 800, 1000 and 1250 Hz and at 3·125 Hz increments for the bands with center frequencies at 1600 Hz, 2000 Hz and 2500 Hz. The energy ratio between the receiving and the excited plates is computed from the test data for the six 1/3 octave frequency bands. In the numerical process presented in this paper the first step is associated with constructing a finite element model for the connection which is being characterized, and utilizing it to compute the power transfer characteristics of each joint. Specifically, the ratio of the total energy stored in the receiving and the excited plate is computed and used as a measurable of the power transfer mechanism. Then, the information for the energy ratio is utilized in the iterative

process to calculate the EFEA power transfer coefficients that represent the particular connection. Finally, the power transfer coefficients are introduced in the EFEA model. The EFEA computations are performed, and the numerical results are compared to the test data. Once the EFEA power transfer coefficients for a particular connection have been computed, they can be utilized in any EFEA model containing the particular connection.

A finite element model is constructed for each plate connection. Based on the material properties for steel and a thickness equal to 0·03 in. the bending wavelength for an infinite plate can be computed as [16]

$$\lambda = c_B/f = \sqrt[4]{D/\rho h}\sqrt{\omega}/f, \tag{25}$$

where c_B is the phase velocity, $D = Eh^3/12(1 - v^2)$ is the rigidity of the plate, h is the plate thickness, ω is the frequency in rad/s and f is the corresponding frequency. For the properties of the fixture utilized in the test, the wavelength at 2500 Hz is 2·08 in. The finite element model is constructed with an average element dimension equal to 0·4 in. It results in approximately five elements per wavelength at 2500 Hz which is just less than the minimum requirement of six elements per wavelength indicated in reference [17]. This is considered sufficient though since a direct frequency response analysis is performed to compute the structural vibration rather than a modal frequency response [17, 18]. The direct frequency response is expected to relax the requirement on the number of elements per wavelength since it eliminates any errors from modal truncation. The finite element model is depicted in Figure 3. The spot-welding is modelled with displacement and rotational constraints imposed at the nodes corresponding to the locations of the

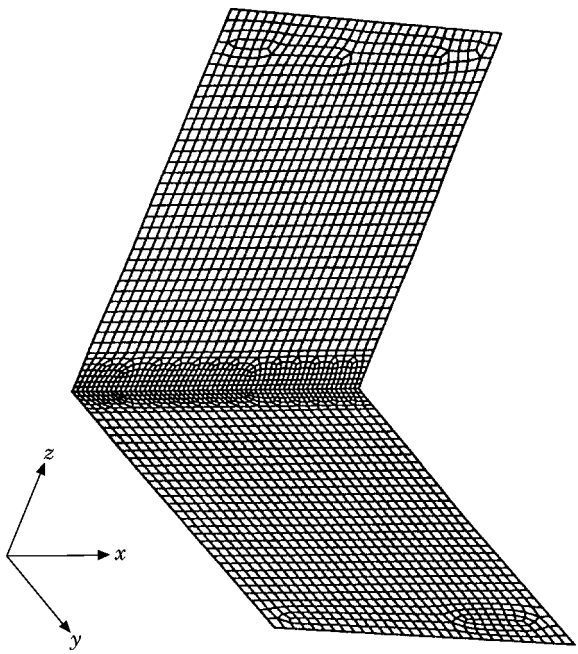

Figure 3. Finite element model for the plate assembly.

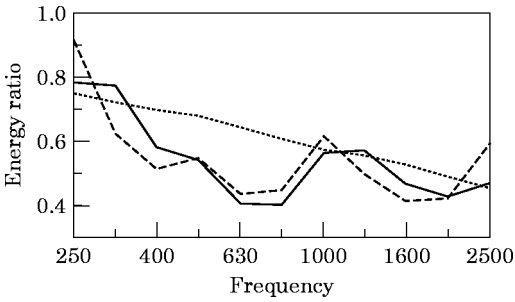

Figure 4. Comparison between test data (—), updated EFEA results (- - -), and baseline EFEA computations (. . . .).

spot-welds. This modelling approach is utilized currently in the low frequency finite element car body models. The averaging algorithm described in section 2.4 is applied to the finite element results. The energy ratio between the receiving and the excited plate is computed. The iterative approach (section 2.5) is employed for evaluating the EFEA power transfer coefficients. The following data are presented:

(1) Test data and numerical results for a set of fully connected plates. Although the work presented in this paper is targeting issues associated with spot-welded connections, the developed approach is also applicable to fully connected joints. Results for fully connected plates over an extended frequency range (250–2500 Hz) are presented. The trends observed in the results presented in this paper for the fully connected plates compare well with trends of other results available in the literature for similar arrangements of fully connected plates [17, 25–27].

(2) Test data and numerical results for the fully connected and the two sets of spot-welded plates in the high frequency range (800–2500 Hz). These results allow one to validate the developed technology for modelling partially connected members, and compare the behavior of fully connected and spot-welded joints.

3.1. FULLY CONNECTED PLATES

A direct finite element frequency response analysis is performed for characterizing the connection between the two plates. The approach presented in section 2·4 is utilized to generate information about the expected energy ratio between the receiving and excited plate. The corresponding EFEA power transfer coefficients are computed through the developed iterative process (section 2·5) and utilized in an EFEA analysis [28]. The original EFEA formulation is also utilized for computations based on power transfer coefficients calculated from analytical solutions of continuously connected semi-infinite members. Results for the energy ratio between the receiving and the excited member are presented in Figure 4. The three curves correspond to test data, EFEA results based on modified power transfer coefficients, and conventional EFEA results based on power transfer coefficients computed by analytical solutions. The following can be observed:

(1) The EFEA analysis that utilizes power transfer coefficients computed by analytical solutions, produces results for the energy ratio between the receiving and the excited plate that decay smoothly with increasing frequency. The observed

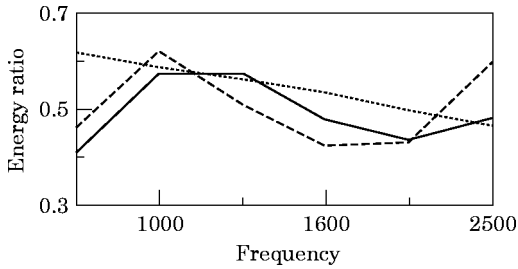

Figure 5. Test data (—), original EFEA solution (. . . .), and modified EFEA solution (- - - -) for fully welded plates.

trend in the results is in agreement with published data for similar configurations computed either by SEA [17, 25, 26] or by EFEA [27].

(2) The energy ratio from test data presents fluctuations with respect to the frequency. Similar behavior can be observed in test or analytical results presented previously for similar assemblies [17, 25–27].

(3) The results from the EFEA analysis that utilizes the modified power transfer coefficients computed by the developed algorithm demonstrate good agreement with the test data. Both the magnitude and the shape of the response curve are captured correctly.

(4) The difference between the EFEA results that utilize power transfer coefficients computed by analytical methods, and the EFEA results that utilize power transfer coefficients computed by the developed methodology is more pronounced at frequencies below 1000 Hz. The latter approach demonstrates good agreement with the test data below 1000 Hz. Therefore, even for continuous connections the power transfer coefficients computed by the developed algorithms seem to improve the accuracy of the EFEA computations.

(5) An analytical solution and SEA results are available in the literature for a similar plate assembly (Figure 6 in reference [25]). Specifically, an exact mathematical solution was developed and a SEA analysis was performed for the vibrations of two thin plates connected at a right angle. The analytical solution presents the same fluctuating behavior with the test data and the EFEA results that utilize the power transfer coefficients computed by the developed method (Figure 4). The SEA results present a smoothly decaying behavior with frequency

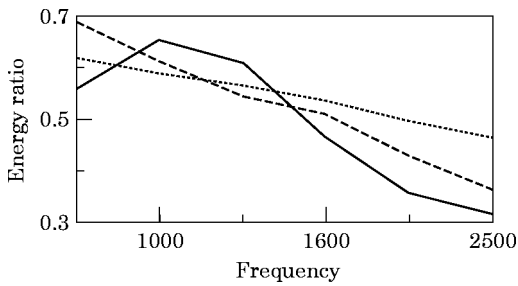

Figure 6. Test data (—), original EFEA solution (. . . .), and modified EFEA solution (- - -) for spot-welded plates at 2 in increments.

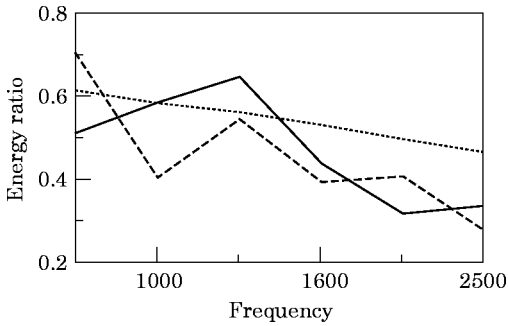

Figure 7. Test data (—), original EFEA solution (. . . .), and modified EFEA solution (- - - -) for spot-welded plates at 4 in. increments.

similar to the EFEA results that utilize power transfer coefficients computed by analytical solutions of semi-infinite members (Figure 4).

3.2. FULLY CONNECTED AND SPOT-WELDED PLATES

The test and numerical results for the three sets of plates are presented in Figures 5–7 for the 1/3 octave bands in the frequency range 800–2500 Hz. The results are presented in terms of the energy ratio between the receiving and the excited plate. Three curves are present in each figure corresponding to: (1) testing; (2) the EFEA analysis that utilizes the power transfer coefficients computed by the developed method (modified EFEA); (3) the EFEA analysis that utilizes power transfer coefficients computed analytically from semi-infinite fully connected members (original EFEA). The following observations are made:

(1) In both test and numerical results from the modified EFEA the fully welded pair of plates demonstrates a more even energy transfer over the entire frequency range.

(2) Both sets of spot welded plates demonstrate decaying energy transfer at higher frequencies. This behavior is captured correctly by the modified EFEA analysis.

(3) Magnitudes of the energy ratio correlate well between test and modified EFEA analysis.

(4) The test data and the modified EFEA results present a similar fluctuating behavior and close correlation, while the original EFEA results demonstrate a smoothly decaying with frequency behavior.

(5) The behavior of the fully welded plates demonstrates increasing energy ratio between the 2000 and 2500 Hz bands. This characteristic is captured correctly by the modified EFEA analysis.

(6) In both test and modified EFEA analysis the spot welded plates present higher energy ratio than the corresponding fully welded pair at some of the lower frequency bands.

The results of the modified EFEA analysis utilize power transfer coefficients computed by the algorithms presented in this paper. Table 1 summarizes the values of the power transfer coefficients computed by this development for the three sets

TABLE 1

Summary of transmission (t) and reflection (r) coefficients between baseline EFEA and modified EFEA solutions

	Baseline		Modified continuous		Modified 2 in. spot-weld		Modified 4 in. spot-weld	
Frequency	*r*	*t*	*r*	*t*	*r*	*t*	*r*	*t*
800	0·665	0·332	0·8	0·2	0·6	0·4	0·575	0·425
1000	0·665	0·322	0·64	0·36	0·655	0·345	0·8	0·2
1250	0·666	0·334	0·72	0·28	0·69	0·31	0·68	0·32
1600	0·666	0·334	0·76	0·24	0·69	0·31	0·78	0·22
2000	0·665	0·329	0·732	0·267	0·73	0·27	0·75	0·25
2500	0·665	0·329	0·53	0·48	0·76	0·24	0·83	0·17

of plates, and the power transfer coefficients computed by analytical solutions of fully connected semi-infinite members. As expected in cases where the targeted energy ratio is lower than the one predicted by the baseline EFEA, the reflection coefficient becomes higher and the transmission coefficient lower. The opposite behavior is observed in the power transfer coefficients when the targeted energy ratio is higher than the baseline. The power transfer coefficients computed for the spot-welded connections are specifically related to the particular spot-welding patterns utilized in this work. The developed algorithm is general and it can be utilized to compute the power transfer coefficients of any spot-welded connection. The power transfer coefficients can be inserted in any EFEA model that includes the corresponding spot-welded connection. The approach developed in this paper does not require to create a non-reflective boundary for any member and thus, it simplifies the testing process for evaluating the energy ratio between receiving and excited member.

4. CONCLUSIONS

An approach has been developed for modelling spot-welded joints in an Energy Finite Element Formulation. It is based on computing power transfer coefficients that reflect the non-continuous nature of the connection. First the energy ratio between a receiving and the excited member is computed from an averaging algorithm and results from conventional FEA analysis. Then the energy ratio information is utilized by an iterative algorithm for evaluating the power transfer coefficients that will make the EFEA model demonstrate a similar energy transfer behavior. The targeted energy ratio between the receiving and excited member may also become available from test data instead of being computed by the averaging algorithm and conventional FEA. In this development there are no requirements to impose artificial damping on any member in order to avoid reflections from the boundaries. The iterative algorithm that computes the power transfer coefficients can accommodate the presence of the reflections from the boundaries. Therefore, a test set up or a conventional FEA model can be simplified. Then the power

transfer coefficients can be computed to capture the prescribed behavior and be utilized by an EFEA model. Three sets of plates are analyzed and tested. Their members are fully connected, spot-welded at 2 in. intervals, and spot-welded at 4 in. intervals. There is good agreement between the test data and results from the developed numerical methodology. The developed approach can be utilized to model non-continuous connections in EFEA or it can be employed to compute power transfer coefficients of fully connected members with increased accuracy.

ACKNOWLEDGMENTS

This work was partially sponsored by Automated Analysis Corporation and Ford Motor Company under contract number 970274. The authors would like to express their gratitude to Alexander Petniunas of Ford Motor Co. for performing the testing in this work.

REFERENCES

1. M. Imai, S. Suzuki, N. Sugiura and H. Sato 1986 *Passenger Car Meeting and Exposition*, *Dearborn*, *MI*, *September SAE Paper* 86411. Radiation efficiency of engine structures analyzed by holographic interferometry and boundary element calculation.
2. M. Hazel, C. Norrey, H. Kikuchi and D. Tres 1996 *SAE International Congress and Exposition*, *Detroit*, *Michigan*, *February SAE Paper* 960145. Using predictive acoustic analysis to evaluate noise issues in under hood applications.
3. D. J. Nefske 1985 *Proceedings of NOISECON* 85, *Columbus*, *Ohio*, *June*, 33–36. Acoustic finite element analysis of the automobile passenger compartment with absorption materials.
4. S. Suzuki 1991 *Boundary Element Methods in Acoustics* (R. D. Ciskowski, C. A. Brebbia, editors). Southampton, Boston: Computational Mechanics Publications; Applications in the Automotive Industry, chapter 7.
5. R. S. Thomas, J. Pan, M. J. Moeller and T. W. Nolan 1997 *Noise Control Engineering Journal* **45**, 25–34. Implementing and improving statistical energy analysis models using quality technology.
6. S. J. Walsh, G. Simpson and N. Lalor 1990 *Proceedings of Inter-Noise* 90, *Gothenburg*, *Sweden*, 961–964. A computer system to predict internal noise in motor cars using statistical energy analysis.
7. R. H. Lyon 1975 *Statistical Energy Analysis of Dynamical Systems*: *Theory and Applications*. Cambridge, Massachusetts: The MIT Press.
8. B. Burkewitz, L. Cohen and F. Baran 1994 *Proceedings of NOISECON* 94, *Ft. Lauderdale*, *Florida*, *May*, 697–702. Application of a large-scale SEA model to a ship noise problem.
9. P. G. Bremner 1994 *Proceedings of NOISECON* 94, *May*, 545–550. Vibro–acoustics of ribbed structure—a compact modal formulation for SEA models.
10. G. A. Rodrigo, M. Klein and G. Borello 1994 *Proceedings of NOISECON* 94, *May*, 887–892. Vibro–acoustic analysis of manned spacecraft using SEA.
11. D. J. Nefske and S. H. Sung 1989 *Journal of Vibration*, *Acoustics*, *Stress and Reliability* **111**, 94–106. Power flow finite element analysis of dynamic systems: basic theory and applications to beams.
12. O. M. Bouthier 1992 *Ph.D. Dissertation*, *Mechanical Engineering Department*, *Purdue University*. Energetics of vibrating systems.
13. O. M. Bouthier and R. J. Bernhard 1995 *AIAA Journal* **30**, 34–44. Models of space averaged energetics of plates.

14. P. Cho 1993 *Ph.D. Dissertation*, *Mechanical Engineering Department*, *Purdue University*. Energy flow analysis of coupled structures.
15. O. M. Bouthier and R. J. Bernhard 1995 *Journal of Sound and Vibration* **182**, 149–164. Simple models of the energetics of transversely vibrating plates.
16. C. Simmons 1991 *Journal of Sound and Vibration* **144**, 215–227. Structure-borne sound transmission through plate junctions and estimates of SEA coupling loss factors using the finite element method.
17. C. R. Fredo 1997 *Journal of Sound and Vibration* **199**, 645–666. A SEA-like approach for the derivation of energy flow coefficients with a finite element model.
18. J. E. Manning 1990 *Proceedings of International Congress in Air- and Structure-Borne Sound and Vibration*, *March*, *Auburn University*, 771–778. Calculation of statistical energy analysis parameters using finite element and boundary element models.
19. K. de Lange, P. Sas and D. Vandepitte 1997 *Journal of Vibration and Acoustics* **119**, 293–303. The use of wave-absorbing elements for the evaluation of transmission characteristics of beam junctions.
20. J. A. Steel and R. J. M. Craik 1994 *Journal of Sound and Vibration* **178**, 553–561. Statistical energy analysis of structure-borne sound transmission by finite element methods.
21. L. Cremer, M. Heckl and E. E. Ungar 1973 *Structure Born Sound*. New York: Springer Verlag.
22. M. A. Gockel [editor], 1983 *MSC/NASTRAN Handbook for Dynamic Analysis*, The MacNeal-Schwendler Corporation.
23. R. S. Langley and K. H. Heron 1990 *Journal of Sound and Vibration* **143**, 241–253. Elastic wave transmission through plate/beam junctions.
24. R. L. Burden, J. D. Faires and A. C. Reynolds 1979 *Numerical Analysis*. Boston, Massachusetts: Prindle, Weber and Schmidt.
25. E. K. Dimitriadis and A. D. Pierce 1988 *Journal of Sound and Vibration* **123**, 397–412. Analytical solution for the power exchange between strongly coupled plates under random excitation: a test of statistical energy analysis concepts.
26. C. Boisson, J. L. Guyader, P. Millot and C. Lesueur 1982 *Journal of Sound and Vibration* **81**, 93–105. Energy transmission in finite coupled plates, part II: application to an L-shaped structure.
27. J. E. Huff and R. J. Bernhard 1995 *Proceedings of Inter-Noise* 95, *Newport Beach*, *July*, 1221–1226. Prediction of high frequency vibrations in coupled plates using energy finite elements.
28. COMET/EFEA *User's Manual*. Ann Arbor, MI: Automated Analysis Corporation.